Received 22 February; accepted 29 April 1988.

1. Binnig, G. & Rohrer, H. *Helv. phys. Acta* **55**, 726–735 (1982).
2. Park, S. I. & Quate, C. F. *Appl. phys. Lett.* **48**, 112–114 (1986).
3. Batra, I. P. *et al. Surf. Sci.* **181**, 126–138 (1986).
4. Hansma, P. K. & Tersoff, J. *J. appl. Phys.* **61**, R1–R24 (1987).
5. Lydon, J. E. & Coakley, C. J. *J. phys. Colloq.* **36**, C1–45 (1975).
6. Cladis, P. E., Bogardus, R. K., Daniels, W. B. & Taylor, G. N. *Phys. Rev. Lett.* **39**, 720–723 (1977).
7. Leadbetter, A. J., Durrant, J. L. A. & Rugman, M. *Molec. Cryst. liq. Cryst.* **34**, 231–235 (1977).
8. Leadbetter, A. J., Frost, J. C. & Gaughan, J. P. *J. Physique* **40**, 375–380 (1979).
9. Pohl, L., Eidenschink, R., Krause, G. & Erdmann, D. *Phys. Lett.* **60A**, 421–423 (1977).
10. Ribotta, R. *J. Phys. Colloq.* **37**, C3–149 (1976).
11. Frommer, J. E. & Chance, R. R. *Encyclopedia of Polymer Science and Engineering* 2nd edn Vol. 5 462–507 (1986).
12. Kaner, R. B. & MacDiarmid, A. G. *Scient. Am.* **258**, 106–111 (1988).
13. Barrall, E. M. & Johnson, J. F. *Liquid Crystals and Plastic Crystals* Vol. 2 (eds Gray, G. W. & Winsor, P. A.) 254–306 (Wiley, New York, 1974).

The weather attractor over very short timescales

A. A. Tsonis & J. B. Elsner

Department of Geosciences, University of Wisconsin-Milwaukee, Milwaukee, Wisconsin 53201, USA

Recent work has used ideas from the theory of dynamical systems in the study of climate and weather over timescales ranging from decades to hundreds of thousands of years[1–5]. In this study, similar ideas are applied to weather observations over a time interval of 11 hours. The results suggest the existence of a low-dimensional strange attractor.

According to the theory of dynamical systems[6], the evolution of a system can be described by trajectories in the state space. The coordinates of the state space are defined by the variables needed to completely describe the evolution of the system. Each trajectory in the state space represents the evolution of the system from some initial condition. If the system exhibits an attractor, all trajectories initiated from different initial conditions will eventually converge and stay on a submanifold of the total available space. This submanifold 'attracts' the trajectories and it is called an attractor. For systems that develop deterministically, their attractors are low-dimensional smooth topological manifolds such as points, limit cycles and toruses. These attractors are, therefore, characterized by an integer dimension that is equal to the topological dimension of the submanifold in the state space. An important property of these attractors is that trajectories converging on them do not diverge, and thus stay at a constant distance from each other. This property guarantees long-term predictability of this system. But the trajectories do not have to stay on a smooth topological manifold. For many dynamical systems it has been found that the trajectories stay on an attracting submanifold that is not topological. These submanifolds are called 'fractal' sets and are characterized by a dimension that is not an integer[7]. The corresponding attractors are called 'strange' attractors. An important property of these attractors is the divergence of initially nearby trajectories. Such an action imposes limits on prediction[8]. Thus, long-term predictability for these systems is not guaranteed. Such systems are then deterministic only in the sense of being described by well behaved differential equations, but they are not periodic or quasi-periodic (even if they are not disturbed irregularly)[9]. Note that the dimensionality of an attractor, whether fractal or not, indicates the minimum number of variables present in the evolution of a system. Therefore, the determination of the dimension of an attractor sets a number of constraints that should be satisfied by a model used to predict the evolution of a system.

In the case where the exact mathematical formulation of the system is not available, the state space can be replaced by the phase space which can be produced using a single record of some observable variable from that system[10,11]. If this system is the atmosphere, for instance, then the observable variable could be the temperature or the pressure or the geopotential. Nicolis and Nicolis[1] were the first to apply the above ideas in climatic studies. Using single-variable values of the oxygen isotope records of deep-sea cores spanning the past million years, they reported a dimension for the climatic attractor equal to 3.1. Fraedrich[2,3] and Essex *et al.*[4] have also analysed weather data over timescales ranging from 15 to 40 years and reported a dimension of the weather attractor between 6 and 7.

Given an observable, say $x(t)$, if the attractor has finite

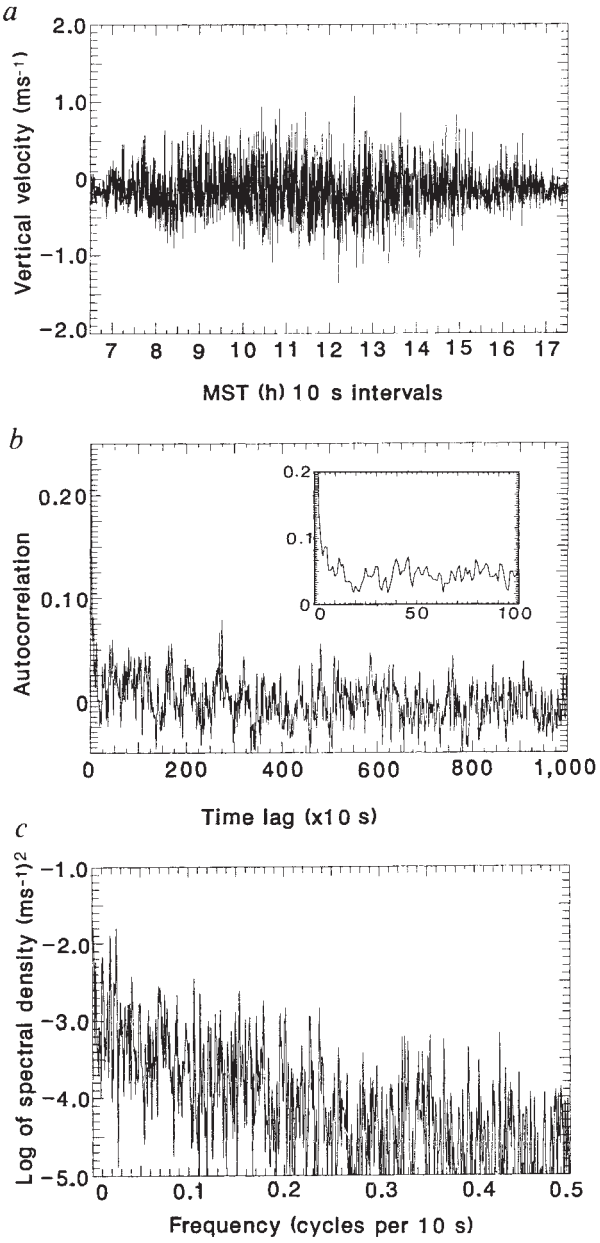

Fig. 1 *a*, The data used in this study represent 10-second averages of the vertical wind velocity over 11 hours. The data were recorded from 0630 to 1730 MST (Mountain Standard Time) on 26 September 1986 at Boulder, Colorado. At about 0630 the sun rises. The air close to the ground is heated and rises, creating strong convection. Positive values indicate updrafts and negative values indicate downdrafts. *b*, The autocorrelation function for the above data. The inset graph is a magnification of the region close to the origin. *c*, The logarithm of the spectral density as a function of the frequency for the above data. The spectra show various peaks on a background of a continuous frequency spectrum. This suggests that a strange attractor may be present.

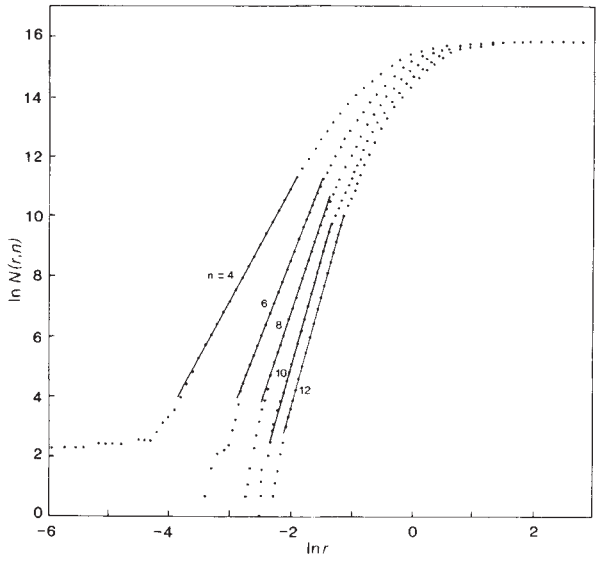

Fig. 2 Plot of ln $N(r, n)$ against ln r for embedding dimensions, $n = 4$, 6, 8, 10, 12. Note the convergence of slopes as n increases.

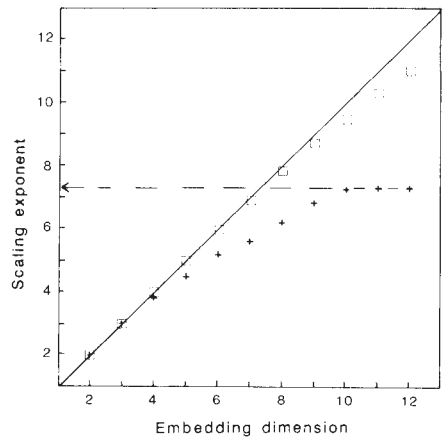

Fig. 3 Scaling exponent, d, as a function of the embedding dimension, n. Crosses correspond to the wind velocity data and squares to a random sample of the same size as the wind data. Note the saturation of the scaling exponent observed for the wind data, although there is no saturation for the random set. From this figure we estimated $d_s = 7.3$.

dimension the complete state vector $\boldsymbol{X}(t)$ can be constructed by the following process[10,11]: $x(t+\tau)$ is used as the first coordinate, $x(t+2\tau)$ as the second ... and $x(t+n\tau)$ as the last, τ being the delay parameter. Thus, for an n-dimensional phase space, a 'cloud' of points will be generated. From this 'cloud' the number of pairs can be found, $N(r, n)$, with distances less than a distance r. If for significantly small r we find that

$$N(r, n) \propto r^d \tag{1}$$

we call d the (correlation) dimension of the attractor for that n (ref. 12). We can then test equation (1) for increasing values of n (the embedding dimension of the phase space). If the value of d becomes independent of n (that is, it reaches a saturation value, d_s), this is evidence that the system represented by the time series should possess an attractor with a dimension equal to d_s; otherwise the time series is random.

It is important to note that when determining the dimension of the attractor (for any embedding dimension of the phase space), only pairs that are separated by a time interval greater than the decorrelation time should be considered. In addition, one should be very cautious in using very few actual data points or highly smoothed data: wrong conclusions can be drawn if the above-mentioned points are not taken into consideration[4,5].

In this work, 10-second averages of the vertical wind velocity recorded 10 metres above the ground over an 11-hour period are analysed. Thus, the total number of points is 3,960. The data are over a timescale much smaller than the previous analyses, and were recorded from 0630 to 1730 MST (Mountain Standard Time) on 26 September 1986 by the National Oceanic and Atmospheric Administration in Boulder, Colorado. Figure 1 shows the data, their autocorrelation and spectral density function. The decorrelation time may be defined as the lag time at which the autocorrelation falls below a threshold value. This threshold value is not uniquely defined, and in general it depends on the problem in hand and the assumptions about the data set. In meteorology this threshold value is commonly defined as $1/e$, especially if the autocorrelation function is nearly exponential[13]. Figure 1*b* (inset) indicates that the autocorrelation function decays nearly exponentially. But in view of the potential problems when correlated pairs are included in the calculations[4,5], we decided to be more conservative. We thus used a decorrelation time that is more 'restrictive' and at the same time allowed us to work with a sufficiently large number of pairs. We adapted a decorrelation time equal to 20 seconds. For time lags greater than 20 seconds, the autocorrelation drops and remains below a value of ~0.10. Figure 2 shows the logarithm of the number of pairs plotted against the logarithm of r for $\tau = 10$ seconds for selected embedding dimensions. From this information for each embedding dimension, the scaling region is determined and its slope is calculated by fitting a straight line in that region. The scaling region is usually observed in the region $3.0 <$ ln $N(r, n) < 11.0$. The slope of the straight line gives the scaling exponent d in equation (1). An excellent discussion about the scaling behaviour of a particular data set and the possible problems associated with fitting a straight line to intervals of r for which r is too large or too small is given by Essex *et al.*[4]. Figure 3 shows this scaling exponent as a function of the embedding dimension, together with a plot representing our time series as a random sample of the same size as our data set. As can be seen in Fig. 3, as n increases, $d \to d_s = 7.3$, but note that no such saturation is observed for the random sample. Therefore, we can conclude that the system represented by the vertical wind velocity series possesses an attractor. The non-integer dimensionality of the attractor indicates that the attracting submanifold is a fractal set and that the attractor is 'strange'.

In that case, the value of d_s suggests that over very short timescales the weather might be represented as a dynamical system with at least eight degrees of freedom (eight differential equations). We thus share the conviction of Nicolis and Nicolis[14] and Essex *et al.*[4] that the atmosphere exhibits properties of a low-dimensional attractor, even though our work refers to a timescale smaller than theirs.

Our analysis was focused on daytime data. During the night the forcing of the Sun is minimum and the wind data do not fluctuate significantly above a mean value of about zero. Thus during a 24-hour interval, the system switches back and forth between dynamical regimes of low and intense activity. Thus, if night-time data are included in the calculation of the correlation dimension, a large number of data points will cluster around one point in the phase space. The result will be an underestimation of the correlation dimension. The above problems are avoided when daytime data are used. The question then arises whether or not the weather attractor over night is of the same dimension as over day, and how the internal dynamics unravel from the day–night cycle. Work in this area is in progress.

It is interesting to speculate on the results reported above. In the early sixties, Lorenz[15] demonstrated that a dynamical system consisting of the three differential equations that give the description of a horizontal fluid layer heated from below exhibits a strange attractor. The warmer fluid formed at the bottom is

lighter and it tends to rise, creating convection currents. This phenomenon takes place in the Earth's atmosphere, where the air close to the ground is heated and rises. This monumental work provided the first mathematically based explanation for the unpredictability of weather. The data analysed here are strongly connected with convection, and the results suggest that in reality the dynamical system that will produce such data should be described by at least eight differential equations, thus being much more complicated and more unpredictable.

Our results support the existence of a low-dimensional attractor, but should be interpreted with caution. As shown in Osborne *et al.*[16], under certain circumstances a stochastic signal may be simulated with a similar structure as some observed data which (stochastic signal) may have a small, finite value for the correlation dimension, even when no underlying attractor is present. Even though this does not necessarily imply that the existence of a small, finite dimension in some observed data is not due to a strange attractor, we think that it is worth mentioning. We hope that research in this area will be beneficial to the debate about the possible existence of low-dimensional attractors in weather and climate or in other systems.

We thank Professors Peter Grassberger and Christopher Essex for discussion, the National Oceanic and Atmospheric Administration and the National Center for Atmospheric Research (NCAR) for providing us with the data and allowing us to use their CRAY computer for our computations, and Ken Hansen for computing assistance.

Received 14 October 1987; accepted 14 April 1988.

1. Nicolis, C. & Nicolis, G. *Nature* **311**, 529–532 (1984).
2. Fraedrich, K. *J. atmos. Sci.* **432**, 419–432 (1986).
3. Fraedrich, K. *J. atmos. Sci.* **44**, 722–728 (1987).
4. Essex, C., Lookman, T. & Nerenberg, M. A. H. *Nature* **326**, 64–66 (1987).
5. Grassberger, P. *Nature* **323**, 609–612 (1986).
6. Holden, A. V. (ed.) *Chaos: an Introduction* (Manchester University Press, 1985).
7. Mandelbrot, B. B. *The Fractal Geometry of Nature* (Freeman, San Francisco, 1982).
8. Crutchfield, J. P., Farmer, J. D., Packard, N. H. & Shaw, R. S. *Scient. Am.* **255**, 46–57 (1986).
9. Grassberger, P. in *Chaos: an Introduction* (ed. Holden, A. V.) 291–311 (Manchester University Press, 1985).
10. Packard, N. H., Crutchfield, J. P., Farmer, J. D. & Shaw, R. S. *Phys. Rev. Lett.* **45**, 712–716 (1980).
11. Takens, F. *Lect. Not. Math.* **898**, 366–381 (1981).
12. Grassberger, P. & Procaccia, I. *Physica* **9D**, 189–208 (1983); *Phys. Rev. Lett.* **50**, 346–349 (1983).
13. Zawadzki, I. *J. appl. Met.* **12**, 459–472 (1973).
14. Nicolis, C. & Nicolis, G. *Nature* **326**, 523 (1987).
15. Lorenz, E. N. *J. atmos. Sci.* **20**, 130–141 (1963).
16. Osborne, A. R., Kirwan, A. D. Jr, Provenzale, A. & Bergamasco, L. *Physica* **23D**, 75–83 (1986).

A guide to Phanerozoic cold polar climates from high-latitude ice-rafting in the Cretaceous

L. A. Frakes & J. E. Francis

Department of Geology and Geophysics, University of Adelaide, GPO Box 498 Adelaide, South Australia, 5001

The high-latitude extent of warm-climate indicators at certain times in Earth history has been considered as evidence that the globe was ice-free for long intervals, despite theoretical considerations and results from numerical modelling experiments[1,2] indicating that this was unlikely. One of the warmest periods, the Cretaceous, displays faunal and floral evidence for 'cool-temperate' to 'sub-tropical' conditions very near to the poles. However, our studies of Lower Cretaceous mudstones of central Australia that contain outsized exotic blocks have led to the conclusion that the blocks were emplaced by ice-rafting, implying that high-latitude ice was present at sea level. Strata of a similar origin of mid-Jurassic to mid-Cretaceous age occur on other continents that were positioned between 65° and 78° palaeolatitude. Indeed, there is a record of high-latitude ice-rafting throughout the Phanerozoic, suggesting that ice was present on Earth for much of its history, and that ice-free conditions could have been at most only episodic over the past 600 Myr.

During the early Cretaceous, central Australia was positioned in mid to high latitudes[3] and was occupied by a large intracratonic basin, the Eromanga Basin, in which marginal sandstones and marine mudstones (the Bulldog Shale) were deposited. The Bulldog Shale of the southwestern Eromanga Basin (Valanginian to Albian in age) is a dark bioturbated or laminated shale with up to 10% sand in its matrix and occasional sandy and silty laminae. It contains large, exotic clasts of mainly Precambrian quartzite and volcanic rock up to 3-m diameter. Clasts occur both as lonestones and as scatterings or concentrations along bedding planes. They show a high degree of rounding and were probably derived from river and/or shoreline environments.

The hydrodynamic paradox presented by the occurrence of outsized boulders in these mudrocks can only be resolved if the clasts were transported laterally into the basin by swift currents or mass-movement processes such as mud flows, or dropped at the depositional site from a floating raft. But strong currents competent to carry large clasts also scour the substrate and deposit layers of sand and coarser material as turbidites, which include erosional surfaces and widespread coarse layers exhibiting graded bedding. Mudflows produce massive non-laminated structures[4]. In contrast, rafted facies are ideally defined by bedding penetrated by the fallen clast; this may only be apparent on the millimetre scale and is often obscured by compaction of mud around the clast. Another important feature of ice-rafted detritus is the sand-sized component known to be present in modern icebergs[5].

Evidence of mass-movement in the form of turbidites or mudflows in the Eromanga Basin is lacking however. Moreover, penetration structures in the laminae below the clasts suggest that the boulders are dropstones, in that they fell vertically from rafts[6], rather than being transported laterally by currents. From sedimentary evidence within the Bulldog Shale, including the presence of glendonites[7–9] and quartz sand grains with surface textures characteristic of glacial regimes, we conclude that ice acted as the rafting mechanism that transported the boulders out into the basin. Although fossil wood is present in the shale and we have considered it as a rafting agent, the large size of

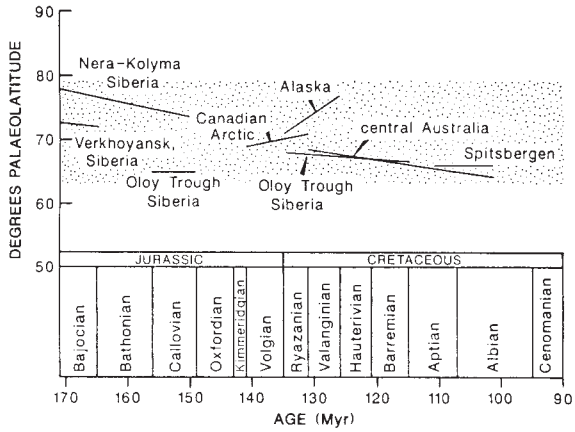

Fig. 1 Distribution of late Mesozoic ice-rafted deposits by palaeolatitude and age. Uncertainties in dating and palaeomagnetic measurements are included in the length of the line for each region. Stippled area (~65–78°) represents full distribution of reported ice-rafted deposits. Palaeolatitudes derived from ref. 26.